Geotechnical and Geophysical Site Characterisation 5 – Lehane, Acosta-Martínez & Kelly (Eds)
 ISBN 978-0-9946261-1-0

Stress-strain response of fine silica sand using a miniature pressuremeter

A.A. Bagbag, J.P. Doherty and B.M. Lehane
School of Civil, Environmental and Mining Engineering, The University of Western Australia

ABSTRACT: The pressuremeter is a well-known geotechnical test, used to measure soil strength and stiffness. In this paper, a miniature pressuremeter device, developed at the University of Western Australia (UWA), was employed to measure the stress-strain behaviour of dense fine silica sand at a range of stress levels. The UWA miniature pressuremeter has a diameter to length ratio of unity, and its inflation after burial in a normally consolidated sand represents a well-defined boundary value problem. Back-analysis was performed using the Finite Element method and the well-known Hardening Soil-Small (HSS) model. The HSS model was found to provide a reasonable match to the measured stress-strain response using parameters derived from triaxial compression tests.

1 INTRODUCTION

Fine 'UWA sand' is a manufactured, uniformly graded silica sand used in geotechnical centrifuge testing at UWA e.g. O'Loughlin and Lehane (2003) Xu and Lehane (2008), Lee, Cassidy, and Randolph (2013). Despite its widespread use, there have been few studies that examine its mechanical properties, with O'Loughlin and Lehane (2003) one of the few studies involving triaxial testing of the sand. More recently, Bagbag et al. (2016) presented results from three anisotropically consolidated drained triaxial compression tests on UWA sand reconstituted to a relative density D_r of 70%.

This paper presents a series of laboratory scale pressuremeter tests on dense UWA sand at a range of confining stresses. The tests were conducted using the UWA miniature pressuremeter described by Johnston et al. (2013). This device is significantly different to any previously built miniature pressuremeter as it uses air as the pressurising fluid and the membrane displacement is measured using strain gauged 'feeler-arm' transducers, rather than inferring displacements from measured volume changes in the pressuring fluid. This direct method of measuring displacement is more accurate than using changes in the fluid volume (Johnston et al., 2013).

The UWA miniature pressuremeter has a diameter to length ratio of unity, and its inflation after burial in a normally consolidated sand represents a well-defined boundary value problem. Therefore, tests were interpreted using available elastic and plasticity solutions based on spherical and cylindrical cavity expansion theory, respectively. The interpreted friction angles, dilation angles and unload reload stiffnesses are presented and compared with data from other tests involving the same sand (Lehane et al. (2005), Xu and Lehane (2008), Lee et al. (2013) and Bagbag et al. (2016)).

The well-defined nature of the boundary value problem provides an opportunity to interpret the pressuremeter tests using the Finite Element (FE) method and sophisticated soil constitutive models. In this paper, the test results are compared with pressuremeter responses calculated using the FE method and the Hardening Soil Small (HSS) model; Plaxis 2D (version 2015.2) was used for the computations (Brinkgreve et al., 2014). The parameters employed for the HSS model were derived in a separate study reported by Bagbag et al. (2016). The aim of this paper is to assess the validity for application to pressuremeter loading of the HSS parameters derived from the triaxial testing.

2 LABORATORY SET-UP

2.1 *Classification data*

'UWA sand' has a minimum and maximum void ratio of 0.45 and 0.75 respectively (Bagbag et al., 2016). The material specific gravity is 2.67 and is classified as a uniform sub-rounded to sub-angular fine sand. The particle size distribution is shown in Figure 1.

2.2 *Preparing and setting-up pressuremeter tests*

A 20 mm diameter laboratory scale pressuremeter developed at UWA by Johnston et al. (2013) was used (see Figure 2a). Unlike previously developed laboratory pressuremeters, the UWA device uses air as the pressurising fluid and the membrane displacement (0.3 mm thick latex) is measured using strain-gauged “feeler-arm” transducers. The pressuremeter was built into an aluminium rod and was located 180 mm above the base of this rod. The rod was positioned at the centre of a 393 mm internal diameter, 400 mm high steel chamber (see Figure 2b, 2c). The top of aluminium rod was clamped to the top of the chamber to prevent it moving during sample preparation and testing (see Figure 2b). Sand was rained into the chamber once the pressuremeter was fixed in place (see Figure 3). The soil density was controlled using an automatic hopper with specific slot widths and heights. Dense sand was achieved by using a slot width of 1.5 mm and the height measured from the sand surface to the opening slot was held constant at 1 m. This produced sand with 70% relative density (void ratio, e = 0.54). The soil filled the chamber with an allowance for a 40 mm thick top plate through which vertical stress was applied to the sand.

A vertical load was applied to the top plate using a hydraulic jack, as shown in Figure 4. This load was applied for a minimum period of 48 hours prior to pressuremeter testing, to allow creep rates to reduce to negligible values (see Lim and Lehane 2014). In this paper, tests are presented for vertical applied pressures of 50 kPa, 60 kPa and 100 kPa.

The pressuremeter device uses a digitally controlled air compressor to expand the membrane. The feeding rate of the pressure was held constant at 50 kPa/min.

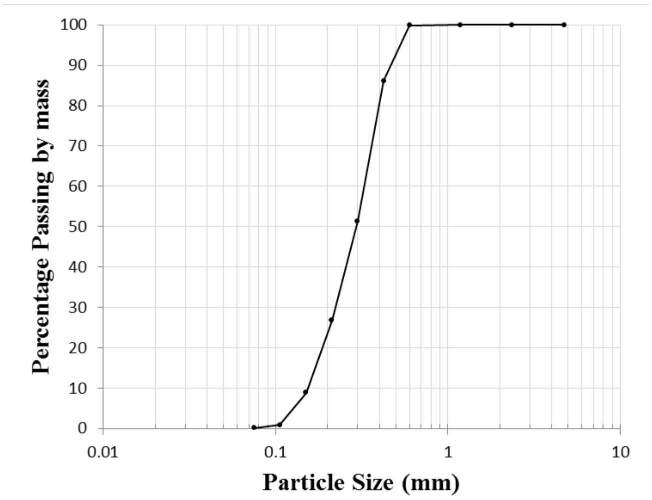

Figure 1. Particle size distribution of UWA fine silica sand

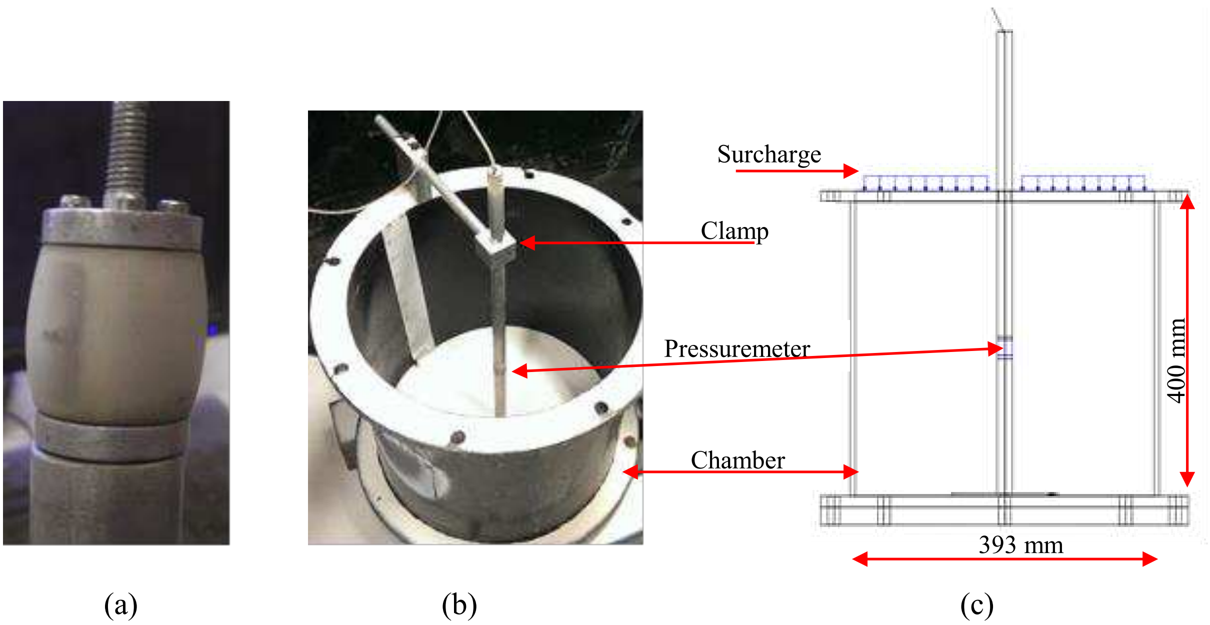

Figure 2. (a) Pressuremeter membrane, (b) pressuremeter in position prior to pouring sand (c) schematic diagram of the experimental set-up.

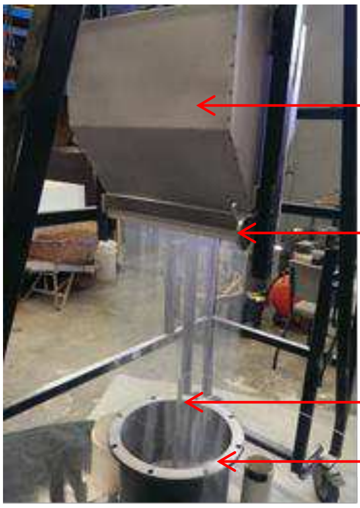

Figure 3. The automatic hopper to rain the sand into pressuremeter chamber test

Figure 4. A typical pressuremeter test setup using a hydraulic system to apply the surcharge load

3 RESULTS AND DISCUSSION

3.1 *Experimental results*

The measured cavity pressure versus corresponding cavity strain for applied vertical stresses of 50 kPa, 60 kPa and 100 kPa are presented in Figure 5a.

Friction (ϕ') and dilation (ψ) angles were estimated using the method of Hughes et al. (1977) as presented in Table 1. This method is based on the slope (s) of a plot of the logarithm of the cavity pressure versus the logarithm of cavity strain (see Figure 5b). An initial estimate of the constant volume friction angle (ϕ'_{cv}) is required. Hughes et al. (1977) proposed equation (1) for friction angle and equation (2) for peak dilation angle. These equations are for cylindrical cavity expansion, which is representative of standard in-situ pressuremeters. The friction and dilation angles inferred using these equations for the three stress levels are presented in Table 1, assuming a ϕ'_{cv} = 34° as recommended for the 'UWA sand' by O'Loughlin and Lehane (2010).

$$\sin \phi' = s/[1+(s-1) \sin \phi'_{cv}] \tag{1}$$

$$\sin \psi = s+(s-1) \sin \phi'_{cv} \tag{2}$$

Table 1. Friction and dilation angles inferred using the Hughes et al. (1977) method for cylindrical expansion.

σ'_v (kPa)	s	ϕ' (degs)	ψ (degs)
50	0.56	47.9	18.2
60	0.51	44.3	13.3
100	0.58	49.1	19.9

Mair and Wood (1987) mentioned that the Hughes et al. (1977) method should be considered approximate, as the friction and dilation angles derived are highly dependent on the estimated value of s. The method also makes the assumption of cylindrical cavity expansion, which is clearly not well suited to the UWA pressuremeter device (given the length/diameter ratio of unity). By comparison with the angles listed in Table 1, the triaxial tests reported by Bagbag et al. (2016) gave an average peak friction angle (ϕ') value of 38.5° and peak dilation angle (ψ) of 10° at the same initial stress level and same relative density of 0.7. Xu and Lehane (2008) deduced peak friction and dilation angles of 42° and 12° for a somewhat denser UWA sand sample at a in-situ stress level of 120 kPa.

Fahey (1991) proposed a method to measure the elastic shear modulus by preforming small unload-reload loops during plastic monotonic loading in pressuremeter tests. These loops exhibit a quasi-linear behaviour and it is suggested that the loop gradient may be used to determine the unload-reload shear modulus from the elastic cavity expansion solutions proposed by Yu (2000). For an assumed elastic response of the soil, the unload-reload shear moduli (G_{ur}) can be determined as:

$$G_{ur} = \Delta p_c/(2k\Delta \varepsilon_c) \tag{4}$$

where Δp_c is the difference between the cavity pressures at the start and end of the unload-reload loop and $\Delta \varepsilon_c$ is the corresponding change in cavity strain; the constant k is 2 for spherical expansion and unity for for cylindrical cavity expansion. As shown in Figure 5a, one test, with an applied vertical stress of 60 kPa, is included an unload-reload loop. Assuming k = 2 (i.e. spherical cavity expansion), the unload-reload shear modulus (G_{ur}) was found to be 25 MPa and 25.8 MPa from the first and second loops, respectively.

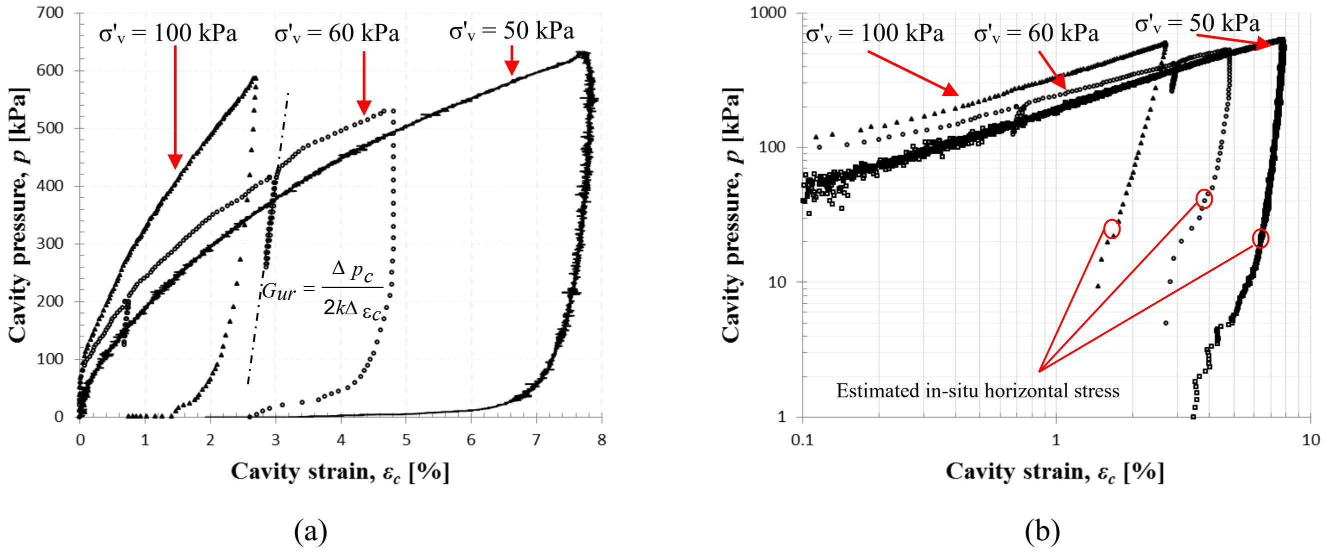

Figure 5. Measured variation of cavity pressure with cavity strain (a) linear scale and (b) logarithmic axes

It is evident from Figure 5 that the lift-off pressure is not easy to distinguish at the start of the tests. However, it is apparent from the final unloading stages that there is a cavity pressure at which the cavity strain reduces rapidly while the cavity pressure remains constant i.e. the unload curve is approximately horizontal. This pressure is likely to be related strongly to the in-situ horizontal stress. The cavity stresses at which this transition occurs can be seen in Figure 5b to be at 20 kPa, 50 kPa and 25 kPa for tests with applied vertical stress of 50 kPa, 60 kPa and 100 kPa respectively, i.e. in average the cavity stresses are approximately half of the applied vertical stress, which is consistent with the expectation that K_0 is approximately 0.5 for the normally consolidated stress history of the sand (see Figure 5).

3.2 *Back analysis*

The Plaxis 2D (version 2015.2) Finite Element program, developed by Brinkgreve et al. (2014), was employed along with the small strain hardening soil model (HSS), introduced by Benz (2007), to simulate the pressuremeter tests. The HSS model soil parameters used are presented in Table 2. These were derived by Bagbag et al. (2016) from consolidated drained trixial tests on 'UWA sand' reconstituted to the same relative density of 0.7 used for the pressuremeter experiments. One of the difficulties encountered by Bagbag et al. was that the secant stiffness at 50% of the peak deviator stress (E_{50}) was found to vary with the stress level raised to the power (m) of 1.0, whereas the very small strain shear stiffness (G_0) was better represented using 'm' an exponent of 0.5. As the HSS model only allows input of a single exponent, the m value was taken equal to 0.5 for the purposes of this paper and the reference stiffness values inputted were those estimated at the average of the three initial lateral stresses in the tests (25 kPa, 30 kPa and 50 kPa). Bagbag et al. (2016) also point out that the shear strain at 70% of the maximum shear modulus ($\gamma_{0.7}$) is stress dependent. As the model does not allow for this stress dependency, the value of $\gamma_{0.7}$ assumed was also taken to be that corresponding to the average of the three initial lateral stresses in the tests.

An axisymmetric model using 687 triangular 15-noded elements was used. The mesh was refined around the membrane as shown in Figure 6. The chamber was modelled assuming a smooth inner surface. The boundary to the right (see Figure 6) was allowed to move vertically, but was fixed radially. The boundary at the base was free radially and fixed vertically. The model includes three major steps: (i) the surcharge pressure was applied in the initial step to establish the initial stresses in the soil with K_0 specified as 0.5, (ii) the pressure was applied to the vertical faces of the pressuremeter to simulate its expansion and (iii) unload-reload loops were applied, as in the physical experiments.

The Plaxis 2D HSS model simulation is presented in Figure 7. The model evidently provides a very good simulation of the measured pressuremeter response at small and medium cavity strains. It may therefore be inferred that the parameters determined from triaxial tests provide a reliable simulation of the pressuremeter tests, especially over the first 2%, which is usually most critical in geotechnical design.

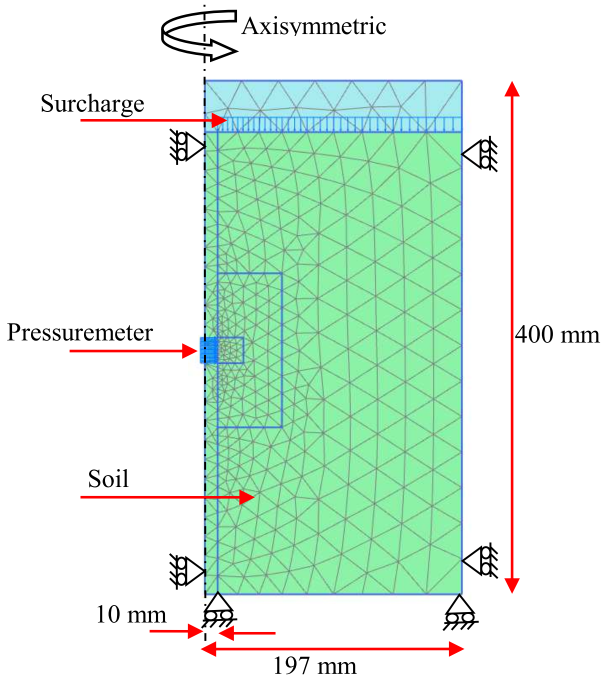

Figure 6. FE model of the experimental pressuremeter test.

Table 2. Hardening Soil Small Parameters

Parameter	Description	HSS
m	Power for stress-level dependency of stiffness	0.5
E_{50}^{ref}	Reference secant stiffness modulus at 50% of the failure load corresponding to the reference stress, p^{ref}	35 MPa
E_{oed}^{ref}	Reference tangent stiffness for oedometer loading modulus corresponding to p^{ref}	35 MPa
E_{ur}^{ref}	Reference unload-reload stiffness modulus corresponding to p^{ref}	105 MPa
c'	Cohesion	0
ϕ	Friction angle	38.5°
ψ	Dilation angle	10°
K_0^{nc}	K_0-value for normal consolidation	0.5
p^{ref}	Reference pressure at which quoted stiffness values apply (taken as atmospheric pressure)	100 kPa
R_f	Failure ratio of deviatoric stress at failure over deviatoric stress at Asymptote	0.9
ν_{ur}	Poissons ratio for unloading-reloading	0.2
$\gamma_{0.7}$	Shear-strain at 70% of small-shear modulus, G_0	2×10^{-5}
G_0^{ref}	Reference small-strain shear modulus	185 MPa

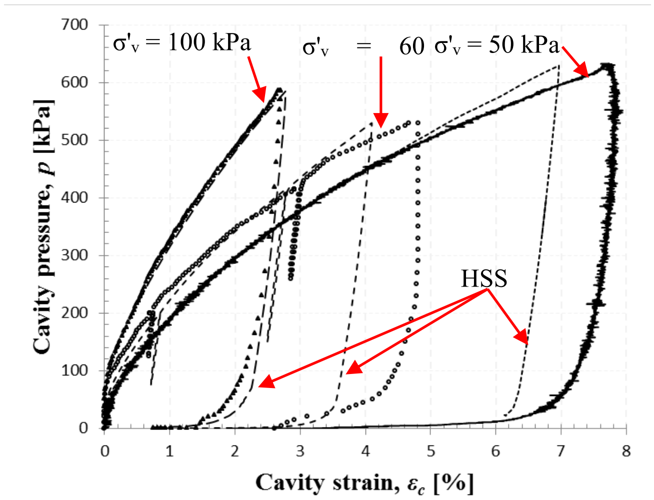

Figure 7. Hardening Soil-Small model for pressuremeter tests.

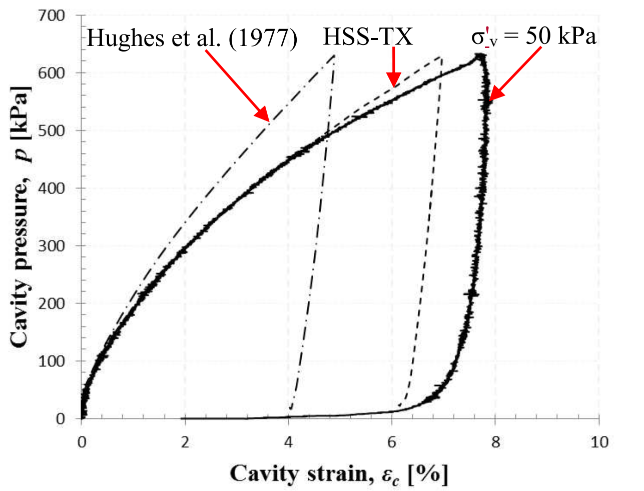

Figure 8. Comparison of measured pressuremeter response at σ'_v = 50 kPa with HSS predictions using triaxial (TX) friction angles and friction angles calculated using Hughes et al. (1977)

Figure 8 explores the sensitivity to friction and dilation angles of the HSS model predictions. All parameters in two sets of analyses (HSS-TX and Hughes et al. (1977) method) were the same except for the friction and dilation angles. The friction and dilation angles for HSS-TX model are presented in Table 2, whereas the angles for Hughes et al. (1977) method are those presented in Table 1 at σ'_v= 50 kPa. It is evident that the triaxial angles provide a better fit to the measurements, which is likely to be, at least in part, due to differences between the near spherical expansion mode in the experiments and the plane strain cylindrical expansion mode assumed in the Hughes et al. (1977) formulation.

4 CONCLUSION

This paper presents results from three laboratory-scale pressuremeter tests performed in reconstituted dense sand. It is shown that, despite its limitations, the Hardening Soil Small model provides a good match to the measured response, when parameters derived from triaxial compression tests are used in the simulations. Further studies are required to understand the differences between the operational friction angles observed in the experiments (where the mode of deformations was approximately spherical) and those back analysed using existing solutions for pressuremeter tests.

5 ACKNOWLEDGEMENTS

The first author would like to acknowledge the sponsorship provided by the King Abdullah Scholarship Program by the Ministry of Higher Education in Saudi Arabia.

6 REFERENCES

Bagbag, A. A., Lehane, B. M., & Doherty, J. P. (2016). Derivation of hardening soil model properties from triaxial tests. *Proc. 26th International Conf. Ocean and Polar Engineering*, Rhodes (Rodos), Greece, ISOPE, *2*, 848-853.

Benz, T. (2007). *Small-strain stiffness of soils and its numerical consequences*: Universität Stuttgart, Institut für Geotechnik.

Brinkgreve, R. B. J., Vermeer, P. A., & Bakker, K. J. (2014). *Material model manual*. Delft: University of Technology & Plaxis BV.

Fahey, M. (1991). Measuring shear modulus in sand with the self-boring pressuremeter. *Proc. 10th European Conference on Soil Mechanics and Foundation Engineering,* Florence, Italy, *1*, 73-76.

Hughes, J. M. O., Wroth, C. P., & Windle, D. (1977). Pressuremeter tests in sands. *Géotechnique, 27*(4), 455-477.

Johnston, G., Doherty, J., & Lehane, B. (2013). Development of a laboratory-scale pressuremeter. *Institution of Civil Engineers, 13*(1), 31-37.

Lee, K. K., Cassidy, M. J., & Randolph, M. F. (2013). Bearing capacity on sand overlying clay soils: experimental and finite-element investigation of potential punch-through failure. *Géotechnique, 63*(15), 1271-1284.

Lehane, B. M., Gaudin, C., & Schneider, J. A. (2005). Scale effects on tension capacity for rough piles buried in dense sand. *Géotechnique, 55*(10), 709-719.

Mair, R. J., & Wood, D. M. (1987). *Pressuremeter testing methods and interpretation*. London: CIRIA / Butterworths.

O'Loughlin, C. D., & Lehane, B. M. (2003). Measurement and prediction of deformation patterns beneath strip footings in sand. *Proc. International Conf. Foundations*, Dundee. British Geotechnical Association, UK, 705-714.

O'Loughlin, C. D., & Lehane, B. M. (2010). Nonlinear cone penetration test-based method for predicting footing settlements on sand. *Journal of geotechnical and geoenvironmental engineering, 136*(3), 409-416.

Xu, X., & Lehane, B. M. (2008). Pile and penetrometer end bearing resistance in two-layered soil profiles. *Géotechnique, 58*(3), 187-197.

Yu, H. S. (2000). *Cavity expansion methods in geomechanics*: Springer Science & Business Media.